Quantized orbits in weakly coupled Belousov-Zhabotinsky reactors

S. Weiss[1,2] and R. D. Deegan[1]

[1] *Center for the Study of Complex Systems, University of Michigan, Ann Arbor, Michigan*
[2] *Institute for Terahertz Science and Technology, University of California, Santa Barbara, California*

PACS 05.45.Xt – Synchronization; coupled oscillators
PACS 82.40.Ck – Pattern formation in reactions with diffusion, flow and heat transfer
PACS 05.45.-a – Nonlinear dynamics and chaos

Abstract – Using numerical and experimental tools, we study the motion of two coupled spiral cores in a light-sensitive variant of the Belousov-Zhabotinsky reaction. Each core resides on a separate two-dimensional domain, and is coupled to the other by light. When both spirals have the same sense of rotation, the cores are attracted to a circular trajectory with a diameter quantized in integer units of the spiral wave length λ. When the spirals have opposite senses of rotation, the cores are attracted towards different but parallel straight trajectories, separated by an integer multiple of $\lambda/2$. We present a model that explains this behavior as the result of a spiral wavefront-core interaction that produces a deterministic displacement of the core and a retardation of its phase.

Higher complexity in nature emerges from interactions between simpler systems [1, 2]. Coupling discrete oscillators, for example, gives rise to large-scale structures such as spiral wavefronts and chimeras [3–6]. The emergence of order in coupled oscillators has been studied in a multitude of geometries [7, 8], in the discrete and continuous limit [5], and with a variety of connectivities [7, 9–11]. In contrast, few studies have explored coupling between spatially-extended systems, despite their importance in nature [12, 13]. Such explorations include synchronisation of turbulent phase- and amplitude fields in coupled one-dimensional complex Ginzburg-Landau equations (cGL) [14], unidirectionally coupled multi-spiral wave patterns generated by a Barkley model [15], or coupling between stationary and oscillating Turing patterns [16]. While all these systems were investigated using numerical tools, the only experimental investigation of coupled spatially extended systems were performed by [17]. They found that coupling of two multi-spiral patterns decreases their spatial disorder, so that only a single or no spiral is left in the asymptotic limit. The same group also conducted simulations, and found that weakly coupling of single spirals results in a coherent motion of their spiral cores, namely circles for co-rotating and straight lines for counter-rotating spirals. This motion was later also observed in coupled cGL by [18].

These large scale spiral core motions are the subject of this paper. We observe for the first time experimentally coherent motion of two coupled spiral cores in a light sensitive Belousov-Zhabotinsky (BZ) reaction. The BZ reaction [19, 20] in two dimensions exhibits spatio-temporal patterns such as spiral or target wave. In the light-sensitive variant [21] the wavefront speed and thus the spiral frequency can be altered with illumination [22], making the BZ reaction an ideal system to study the coupling of spatially extended oscillating systems.

We also utilize numerical simulation to investigate the large scale motion. We find that when spirals share the same sense of rotation, their cores move along a common circular path with a diameter quantized to integer multiples of λ where λ is the distance between crests of a spiral wavefront along the radial direction originating from the core. When the spirals have opposite sense of rotation their cores move on different but parallel straight trajectories separated by integer multiples of $\lambda/2$. We developed a deterministic model that reproduces these quantized orbits based on the simple premise that each wavefront crossing a core perturbs the core position and phase. Quantized obits are limit cycle attractors within this model.

In our numerical simulations we integrate the two-variable Oregonator model [23, 24] with forcing (see e.g.

[25,26]):

$$\partial_t u_i = \nabla^2 u_i + \frac{1}{\epsilon}\left[u_i - u_i^2 - (f v_i + I_i)\frac{u_i - q}{u_i + q}\right] \quad (1)$$

$$\partial_t v_i = 0.5\nabla^2 v_i + u_i - v_i \quad , \quad (2)$$

using an Euler scheme on a two-dimensional (580×580) large grid with time steps $\Delta t = 0.001$ and grid spacing $\Delta x = 0.2$. Here u is the concentration of the autocatalytic reactant hydrobromous acid ($HBrO_2$), v is the concentration of the oxidized catalyst ($Ru(bpy)^{3+}$), I is the additional bromide production induced by illumination, and i stands for the domain number 1 or 2. The other parameters are constants that depend on the concentration of other chemical species and their reaction rates. These are fixed at $q = 0.0015$, $\epsilon = 0.08$ and $f = 1.5$ in all our simulation. While more sophisticated models are available [27,28], this implementation of the Oregonator is only qualitatively accurate. The catalyst is mobile, and Eq. 2 includes a diffusive term with a diffusivity estimated from the molecular mass of $Ru(bpy)^{3+}$. For these parameters the Oregonator can support either a uniform oscillatory state or spirals undergoing rigid rotation. However, since the spiral frequency is faster, once a spiral nucleates it overruns any areas with homogenous oscillations.

The forcing term $I_i(\vec{x}, t)$, was calculated as follows:

$$I_i(\vec{x}, t) = I_0 \cdot H(v_j(\vec{x}, t) - v_t), \quad \text{with} \quad i \neq j, \quad (3)$$

where I_0 is the coupling strength, $H(x)$ is the Heaviside function and v_t is a threshold value $(v_{min} + v_{max})/2$ where v_{min} and v_{max} are the extreme values of v during a single cycle in the unforced homogeneous Oregonator model.

In our experiments we used a Ruthenium complex compound Tris (bipyridyl) dichlororuthenium ($Ru(bpy)^{2+}$) as the catalyst. It absorbs light with wavelength $\approx$ 450 nm, opening a production channel for the inhibitor (Br^-) [22, 27]. The reaction ran in a continuously fed stirred tank reactor (CSTR) [29–32], consisting of two chambers connected by a 0.5 mm thick, 19 mm diameter porous glass membrane (Vycor) into which reactants from both chambers slowly diffuse, meet, and react. Thus, the reaction occurs exclusively within the membrane. One chamber was supplied with an aqueous solution of sodium bromide (NaBr), malonic acid, sulfuric acid (H_2SO_4), and sodium bromate ($NaBrO_3$) with respective concentrations 0.02 M, 0.1 M, 0.5 M, 0.15 M; the other was supplied with aqueous solution of $Ru(bpy)^{2+}$, H_2SO_4, and $NaBrO_3$ with respective concentrations 0.5×10^{-3} M, 0.5 M, 0.15 M. Peristaltic pumps continuously fed fresh reactants into each chamber and removed reaction products, thus keeping the concentrations of reactants constant in each chamber.

Two distinct circular domains of equal diameter ($\approx$ 9 mm) were defined on the membrane by shinning light outside these areas with a large intensity. This ensured, that waves originating in one domain could not enter into the other. We call these domains cell 1 and cell 2. The light from the projector is filtered with a shortpass filter ($\lambda_{light} < 475$ nm) before striking the reactor. Before each experimental run, in each cell we coaxed the formation of a single spiral with a predefined core location by projecting a slowly rotating Archimedean spirals.

The cells were coupled by a camera and video projector system. The image of one cell was captured with a monochrome camera (PixeLink PL-E531MU), binarized, and projected (Optoma TX542) back onto the other cell, and vice versa. In each cycle the threshold was reset to the 60th percentile of the intensity distribution. During image capture a diffuser was placed in front of the projector and the output of the projector was set to a uniform image dimmed to the minimum level. Since the filtered light is absorbed by $Ru(bpy)^{2+}$ but not $Ru(bpy)^{3+}$, the $Ru(bpy)^{2+}$-rich regions appeared dark in transmission whereas the $Ru(bpy)^{2+}$-poor ($Ru(bpy)^{3+}$-rich) regions appeared bright. The duration of each cycle - and thus the refresh time of the projected image - was typically less than two seconds, which is small in comparison to a typical 40 s spiral period. Thus, we don't expect the capture-projection cycle to introduce additional forcing to the system.

We find in experiments and simulations that spirals with the same sense of rotation are attracted to a circular limit cycle (see Fig. 1). [17] observed similar phenomena in simulations but with a different coupling scheme. Initially the cores exhibit a transient, particularly clear in simulations, before settling on a limit cycle. In simulations the limit cycles in both cells are identical, whereas in experiments they exhibit small differences that we attribute to inhomogeneities in the membrane and misalignment of the optical system.

The trajectories in the xy-plane are well described by

$$x(t) = x_0 + R\cos(\Omega t + \Theta_0) + r\cos(\omega t + \psi_0)$$
$$y(t) = y_0 + R\sin(\Omega t + \Theta_0) + r\sin(\omega t + \psi_0), \quad (4)$$

where R, Ω and Θ_0 are the radius, rotational frequency and phase of the large revolution, and r, ω and ψ_0 denote the same quantities for the small but faster cycloidal motion. Here we focus on R, Ω and Θ_0.

We conducted multiple simulations with a range of initial core-to-core separation distances d_0, tracked the core positions, and fit these to eq. 4. In all cases the phase difference was $\Theta_0^{(1)} - \Theta_0^{(2)} = \pi$. Thus, at any moment the cores are on opposite sides of the circular limit cycle and always $2R$ apart.

Figure 2(a) shows that R and Ω vary in discrete steps with d_0. R and Ω are near enough equal in both cells so that their differences are nearly indistinguishable in the plot. R increases in steps of size $\Delta R = 9.2 \pm 0.1$ with increasing d_0. This value is close to half the wavelength of the coupled spiral $\lambda \approx 18$, though we note that the spiral is distorted and the wavelength is ambiguous. The wavelength of uncoupled spirals is clear and equals 15.

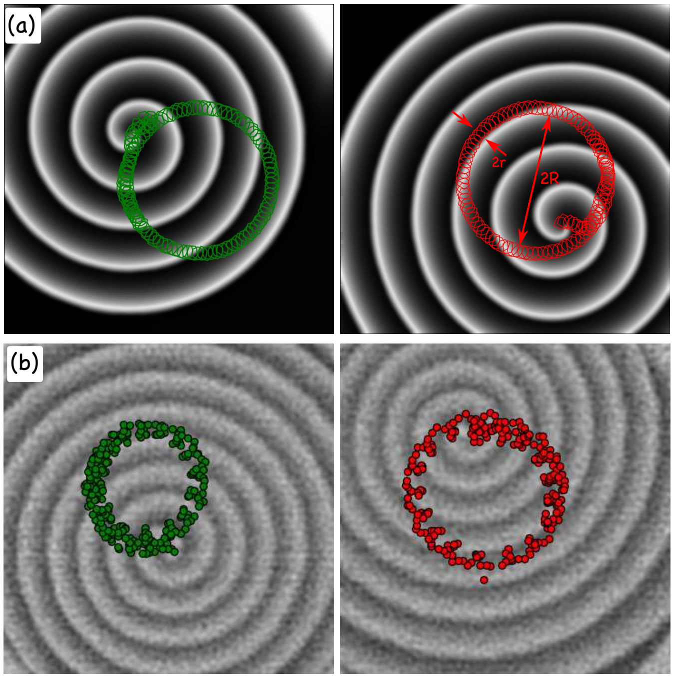

Fig. 1: Trajectories of weakly coupled spirals with the same sense of rotation in simulations (a) and experiments (b). The background patterns show the initial pattern before the coupling is turned on. The arrows indicate the parameters r and R from eq. 4.

But coupling causes the wavelength to increase (due to the smaller rotation frequency) and the ensuing motion causes a doppler-like compression and dilation of the wavelength along the direction of motion. Ω is also quantized and decreases with d_0, and is has the same sign as ω, indicating that the cores move in the same direction as the spiral rotation. Fig. 2(b) shows that Ω varies inversely with R; a power law fit yields $\Omega \propto R^{-0.8\pm0.1}$.

Spirals with opposite sense of rotation move along straight parallel trajectories, as shown in fig. 3. Similar behavior was also observed in simulations by [17]. We conducted multiple simulations with different initial separation distances d_0 and found a similar quantization of the separation distance (see Fig. 4). The difference between plateaus is $d_n - d_{n-1} = 9.3 \approx \lambda/2$. We see in Fig. 4, that d can take different values for the same d_0, since it does also depend on the initial phases ψ_0.

The quantization of the trajectories is recovered from a model based on the idea by [33] that a short light pulse causes a displacement h of the spiral core and a phase lag $\delta\theta$. We approximate the spiral as a counterclockwise rotating Archimedian spiral

$$\theta = -\frac{2\pi r}{\lambda} + \theta_0(t) \quad \text{with} \quad \theta_0(t) = \psi_0 + \omega t, \tag{5}$$

where ψ_0 and ω are the same as in eq. 4. We assume that passage of a wavefront from spiral #1 across the core of #2 (and vice versa) is equivalent to Zykov's short light-pulse. Therefore, after k such wavefronts

$$\theta_0(t) = \psi_0 + \omega t - k \cdot \delta\theta. \tag{6}$$

We also assume that the light pulse shifts the spiral core location $z = x + iy$ by δz. The direction of the shift depends on the instantaneous spiral phase. Following [33], we code the directionality using $\delta z = h \exp(i\varphi + i\theta_0(t))$. After $k+1$ pulses the core's location is

$$z_{k+1} = z_k + h \exp\left[i(\varphi + \psi_0 - k \cdot \delta\theta + \omega t)\right] \tag{7}$$

We first consider two counter-clockwise rotating spirals with their cores at positions $z^{(1)}$ and $z^{(2)}$. Spiral #1 experiences a light pulse whenever an arm from spiral #2 passes $z^{(1)}$. This condition is met when $\theta^{(2)} = arg(z^{(1)} - z^{(2)}) + 2\pi n_1$ with $\theta^{(2)}$ specified by eq. 5, where n_1 is any integer, and $r = |z^{(1)} - z^{(2)}|$. For spiral #2 the expression is the same with $1 \to 2$ and $2 \to 1$. Under the assumption that the frequencies of both spirals (ω) are the same[1], combining this with eq. 6 yields :

$$\psi_0^{(j)} - k\delta\theta - \frac{2\pi|z^{(l)} - z^{(j)}|}{\lambda} + \omega t_j = arg(z^{(j)} - z^{(l)}) + 2\pi n_l \tag{8}$$

where $j, l \in \{1, 2\}$ and $j \neq l$. t_j is the time when core j is hit by a wavefront from core l. Solving 8 for ωt_1 and ωt_2, inserting the result into 7, and substituting $\Delta\psi = \psi_0^{(1)} - \psi_0^{(2)}$ and $\Delta z_k = z_k^{(1)} - z_k^{(2)}$, the location of the jth core after $k+1$ pulses is: Note, the introduction of the Kronecker delta δ_{j2} which originates from the relation $arg(-\Delta z_k) = arg(\Delta z_k) + \pi$. Thus the vector between core #1 and #2 is

$$\Delta z_{k+1} = \Delta z_k + \delta\Delta z_k \quad \text{with}$$
$$\delta\Delta z_k = 2h \cdot \cos(\Delta\psi) \exp[i(\varphi + arg(\Delta z_k) + \frac{2\pi}{\lambda}|\Delta z_k|)]) \tag{10}$$

We now analyze the map given by Eq. 10. First we note that for the special case of $\Delta\psi = (2n+1)\pi/2$ ($n \in \mathbb{Z}$), Δz_k is constant for all times and k. For other values of $\Delta\psi$, the dynamics are more interesting. We look for solutions of Eq. 10 with constant core-to-core distance $|\Delta z|$. These occur when $\delta\Delta z_k$ is perpendicular to Δz_k:

$$\varphi + arg(\Delta z_k) + \frac{2\pi}{\lambda}|\Delta z_k| = arg(\Delta z_k) + \frac{\pi}{2} + m\pi. \tag{11}$$

Solving for $|\Delta z_k|$:

$$|\Delta z_{k_0}| = \frac{\lambda}{2\pi}(-\varphi + \pi/2 + m\pi). \tag{12}$$

Eq. 12 shows already the quantization of $|\Delta z|$ and thus also of R. However, not all of these steady solutions are

[1]This is most certainly true since they are produced with the same parameters. In addition, we have assumed that k is the same for both spirals as well. This is also a valid assumption, because its number depends on the rotation frequency ω, which is the same for both spirals.

$$z_{k+1}^{(j)} = z_k^{(j)} + h \cdot \exp\left[i(\varphi - \cdot(-1)^j \Delta\psi + arg(\Delta z_k) + \pi\delta_{2j} + \frac{2\pi}{\lambda}|\Delta z_k|)\right]. \tag{9}$$

stable. One can show, that for $\cos(\Delta\psi) > 0$ [$\cos(\Delta\psi) < 0$], solutions are stable [unstable] for $m = 0, 2, 4 \ldots$, but are unstable [stable] for $m = 1, 3, 5 \ldots$ [2]. In any case, only clockwise rotation of Δz_k are stable, *i.e.* the same sense as the spiral rotation. Thus, the difference between two stable trajectories is $|\Delta z(m+1)| - |\Delta z(m)| = \lambda$. This agrees with our observation that the radii of successive limit cycles differ by $\lambda/2$. Now we can calculate the parameter φ (by using eq. 10) to be $\varphi = -0.50$. We point out, that the relation $|\Delta z = 2R|$ assumes that the center point $(z_k^{(1)} + z_k^{(2)})/2$ is constant. One can show from 9 that this is true for $\cos(\Delta\psi) = \pm 1$. While the presented model here treats $\Delta\psi$ as an initially given parameter, in the simulation we observe that after the initial transient, the spirals have fixed phase relations of either $\Delta\psi = 0$ or $\Delta\psi = \pi$.

Note, that eq. 10 suggests a constant velocity along the trajectory, such that $\Omega \propto R^{-1}$, whereas we find in simulations that $\gamma \approx -0.8$. We attribute the discrepancy to the difference in the coupling. While the model assumed an infinitely short light pulse, the forcing schemes in the simulation produces spatially extended regions close to the wavefront maxima. Wave fronts further away from the spiral core travel slower (due to their smaller curvature) and thus cause a longer forcing to the other spirals core.

Applying the same reasoning to counter-rotating spirals, we arrive at an expression for the difference vector between cores:

$$\Delta z_{k+1} = \Delta z_k - 2h \cdot \cos(\varphi + \frac{2\pi}{\lambda}|\Delta z_k|) \exp[i(\Delta\psi - arg(\Delta z_k))] \tag{13}$$

From eq. 13, we see, that Δz is constant for all k if

$$|\Delta z_{k_0}| = \frac{\lambda}{2\pi}\left(-\varphi + \pi/2 + m\pi\right) \quad \text{with} \quad m \in \mathbb{Z}. \tag{14}$$

Eq. 14 shows the same quantization of the spiral distances as eq. 12. However, now the amplitude of $\delta\Delta z$ vanishes and thus Δz does not change at all. In addition, the stability of the steady solution (eq. 14) depends only on $\Delta\psi - arg(\Delta z_k)$ and therfore, one finds stable solutions for any m. Note, that with eq. 14 fullfilled, only Δz is steady, whereas z_1 and z_2 move parallel to each other. We show the steady solutions of eq. 14 as red lines in fig. 4. For this we used $\varphi = -0.50$ as calculated from the case of two co-rotating spirals. We see, that there is a small discrepancy between the results from simulation (blue points) and the model prediction (red lines), which increases with increasing m. We attribute this discrepancy to the infinite small pulse time assumed in the model in contrast to the finite forcing time in the simulations.

[2]See suplementary material.

Here we presented simulations and experiments on the coupling of spatially extended oscillating media. Weak coupling of two spirals leads to a synchronized large scale motion of their cores. Co-rotating spirals move on circular trajectories with diameters equal to integer multiples of the spiral wavelength and counter-rotating spirals move along straight trajectories parallel to each other, separated by integer multiples of half the wavelength. A theoretical model that assumes a small change of the spiral phase and the spiral core location whenever a wavefront of one spiral hits the core location of the other explains well the motion of the coupled spirals and the observed quantization of their relative core distance.

* * *

We acknowledge fruitful discussions with V. Zykov. We are also grateful to Harry Swinney for the gift of the Vycor disks, and to the James S. McDonnell Foundation for support. SW acknowledges financial support by the Deutsche Forschungsgemeinschaft.

REFERENCES

[1] Anderson P., *Science*, **177** (1972) 393.
[2] Laughlin R. B. and Pines D., *Proceedings of the National Academy of Sciences*, **97** (2000) 28.
[3] Perez-Munuzuri A., Perez-Munuzuri V., Perez-Villar V. and Chua L., *Circuits and Systems I: Fundamental Theory and Applications, IEEE Transactions on*, **40** (1993) 872.
[4] Abrams D. M., Mirollo R., Strogatz S. H. and Wiley D. A., *Phys. Rev. Lett.*, **101** (2008) 084103.
[5] Martens E. A., Laing C. R. and Strogatz S. H., *Phys. Rev. Lett.*, **104** (2010) 044101.
[6] Martens E. A., Thutupalli S., Fourriére A. and Hallatschek O., *PNAS*, **110** (2013) 10563.
[7] Watts D. J. and Strogatz S. H., *Nature*, **393** (1998) 440.
[8] Acebrón J. A., Bonilla L. L., Pérez Vicente C. J., Ritort F. and Spigler R., *Rev. Mod. Phys.*, **77** (2005) 137.
[9] Blasius B., Huppert A. and Stone L., *Natue letters*, **399** (1999) 354.
[10] Boccaletti S., Kurths J., Osipov G., Valladares D. and Zhou C., *Physics Reports*, **366** (2002) 1.
[11] Pikovsky A., Rosenblum M. and Kurths J., *Synchronization - A universal concept in nonlinear science* (Camb) 2003.
[12] Danø S., Sørensen P. G. and Hynne F., *Nature*, **402** (1999) 320.
[13] Glass L., *Nature*, **410** (2001) 277.
[14] Boccaletti S., Bragard J., Arecchi F. T. and Mancini H., *Phys. Rev. Lett.*, **83** (1999) 536.

[15] Berg S., Luther S. and Parlitz U., *Chaos: An Interdisciplinary Journal of Nonlinear Science*, **21** (2011) .

[16] Yang L. and Epstein I., *Phys. Rev. Lett.*, **90** (2003) 178303.

[17] Hildebrand M., Cui J., Mihaliuk E., Wang J. and Showalter K., *Phys. Rev. E*, **68** (2003) 026205.

[18] Nie H., Gao J. and Zhan M., *Phys. Rev. E*, **84** (2011) 056204.

[19] Belousov B. P., *Sbornik Referatov po Radiatsionnoi Meditsine za 1958 god*, (1958) 145.

[20] Zaikin A. N. and Zhabotinsky A. M., *Nature*, **225** (1970) 535.

[21] Demas J. N. and Diemente D., *Journal of Chemical Education*, **50** (1973) 357.

[22] Petrov V., Ouyang Q., Li G. and Swinney H. L., *The Journal of Physical Chemistry*, **100** (1996) 18992.

[23] Field R. J., Koros E. and Noyes R. M., *Journal of the American Chemical Society*, **94** (1972) 8649.

[24] Field R. J. and Noyes R. M., *The Journal of Chemical Physics*, **60** (1974) 1877.

[25] Zykov S., Zykov V. and Davydov V., *EPL (Europhysics Letters)*, **73** (2006) 335.

[26] Krug H. J., Pohlmann L. and Kuhnert L., *The Journal of Physical Chemistry*, **94** (1990) 4862.

[27] Kiádár S., Amemiya T. and Showalter K., *The Journal of Physical Chemistry A*, **101** (1997) 8200.

[28] Nakata S., Matsushita M., Sato T., Suematsu N. J., Kitahata H., Amemiya T. and Mori Y., *The Journal of Physical Chemistry A*, **115** (2011) 7406 pMID: 21563834.

[29] Ouyang Q. and Swinney H. L., *Chaos: An Interdisciplinary Journal of Nonlinear Science*, **1** (1991) 411.

[30] Ouyang Q. and Flesselles J.-M., *Letters to Nature*, **379** (1996) 143.

[31] Belmonte A. L., Ouyang Q. and Flesselles J.-M., *J. Phys. II France*, **7** (1997) 1425.

[32] Martinez K., Lin A. L., Kharrazian R., Sailer X. and Swinney H. L., *Physica D: Nonlinear Phenomena*, **168-169** (2002) 1 .

[33] Zykov V. and Engel H., *Analysis and Control of Complex Nonlinear Processes In Physics, Chemistry and Biology* (World Scientific) 2007 Ch. Unified approach to feedback-mediated control of spiral waves in excitable media.

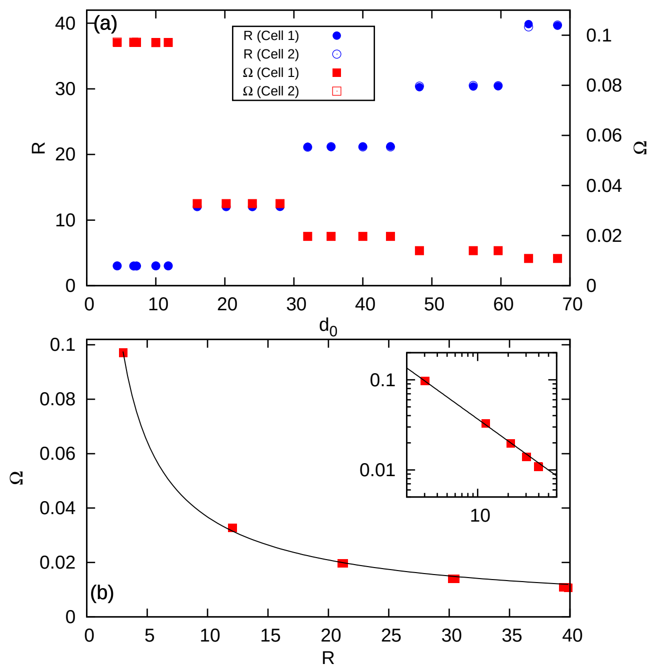

Fig. 2: Slow rotation as a function of the initial separation distance between the spiral core in cell 1 and the spiral core in cell 2. (a): Radius R of cell 1 (blue solid bullets) and of cell 2 (blue open circles) as a function of the initial separation distance (left y-axis). Also shown is the frequency Ω for spiral core rotation in cell 1 (red solid squares) and cell 2 (red open squares). (b): Ω as a function of R. The solid line is a power law fit with exponent $\gamma = -0.8$. The insert shows the same data plotted on a log-log plot.

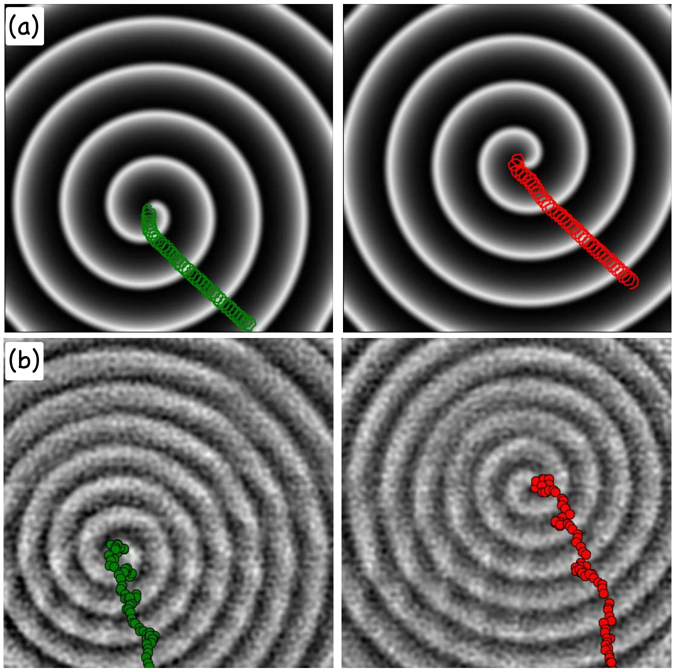

Fig. 3: Weak coupling of two spiral, rotating in opposite directions. Shown are results from simulations (a) and from experiment (b, images are digitally enhanced). The gray images show the initial patterns. The blue and red curves mark the trajectories of the spiral cores

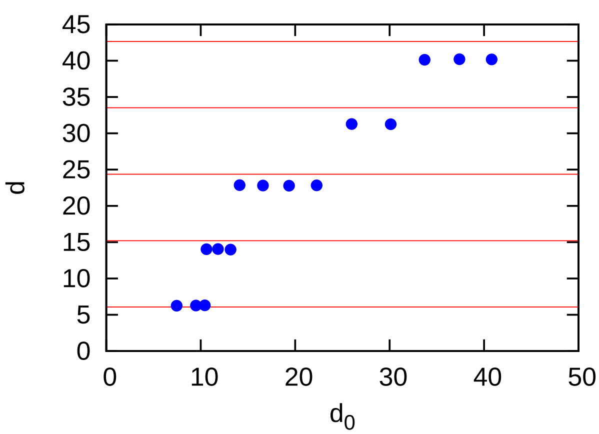

Fig. 4: Final separation distance d as a function of the initial separation distance d_0 for counter-rotating spirals. Red horizontal lines mark predictions by eq. 14, with φ and λ calculated from the case of two spirals with the same orientation.